Int J Clin Exp Med 2016;9(6):10265-10272
www.ijcem.com /ISSN:1940-5901/IJCEM0022663

Original Article

The preparation of reduced graphene oxide and its photothermal therapy of gliomas *in vivo* and *in vitro*

Hai-Sheng Wang[1], Hong-Xia Chen[2], Yue-Hong Ma[3]

[1]College of Basic Medical Sciences, Inner Mongolia Medical University, Jinshan Development Zone, Hohhot, Inner Mongolia Autonomous Region, China; [2]The Second Hospital of Chaoyang District, Beijing, China; [3]Pharmacology Teaching and Research Division, College of Basic Medical Sciences, Inner Mongolia Medical University, Jinshan Development Zone, Hohhot, Inner Mongolia Autonomous Region, China

Received December 24, 2015; Accepted April 6, 2016; Epub June 15, 2016; Published June 30, 2016

Abstract: Objective: To investigate the preparation of reduced graphene oxide (reduced-NGO) and its photothermal therapy of gliomas *in vivo* and *in vitro*. Methods: Hydrazine hydrate reduction method was used to reduce graphene oxide (NGO). The morphology, diameter, stability and UV-VIS absorbance of reduced-NGO were detected firstly; and then, the photothermal conversion effect of reduced-NGO under 2 w/cm^2 808 nm irradiation was tested. MTT method was used to detect the effect of reduced-NGO alone and reduced-NGO combined with 808 nm near-infrared laser (NIR) irradiation on cell viability. Lastly, the photothermal therapeutic effect of reduced-NGO for treating U87 tumor *in vivo* was detected. Results: Reduced-NGO obtained by hydrazine hydrate reduction method was lamellar particle with a diameter of 90 nm, which showed strong NIR absorbance, great stability and biocompatibility. The temperature of reduced-NGO solution could reach 70°C under 2 w/cm^2 808 nm irradiation for 5 min. Reduced-NGO combined with 2 w/cm^2 808 nm irradiation could significantly inhibit cell viability and tumor growth. Conclusion: Herein, we successfully synthesized reduced-NGO which showed good tumor killing effect *in vitro* and *in vivo* and no toxicity when combined with 808 nm radiation.

Keywords: Reduced-NGO, glioma U87 cell, photothermal therapy, hydrazine hydrate

Introduction

Graphene was a two dimensional carbon material piled up by single layers of carbon atoms. With its unique electrical, optical, mechanical and thermal properties, it had a broad application prospect in the field of biology, medicine and composite material [1-5]. Graphene oxide (NGO) was usually prepared by oxidation of graphene. The structure of graphene oxide was generally the same as graphene except for some oxygen-containing functional groups, such as epoxy group, hydroxyl and carboxyl [6-9]. In this way, the water solubility of graphene was enhanced.

Reduced-NGO, a derivative of NGO, could be prepared by using NGO via chemical or physical methods [10, 11]. Through reduction, some oxygen-containing functional groups on the surface of NGO could be removed, π-π conjugated system on the surface of NGO and NIR absorption intensity of NGO could be improved. In recent years, because of the large specific surface area of graphene and its derivative, it could not only load various biomolecules but also pure metal and metal compounds with abundant functions to prepare functional nano composites based on graphene [12-14]. A large number of toxicity tests showed that surface-modified graphene had no obvious toxicity for both cells and mice. In addition, graphene was of its unique optical property. Its strong absorbance in near-infrared region made it applicable in the photothermal therapy of tumors *in vivo* [15-17].

In this study, reduced-NGO was synthesized by hydrazine hydrate reduction method. By taking advantage of its optical property, we applied it to the photothermal therapy of gliomas *in vivo* and *in vitro*.

Methods and materials

Experimental materials

Hydrazine hydrate was purchased from Sigma (the US), NGO platelets from ACS Material (the

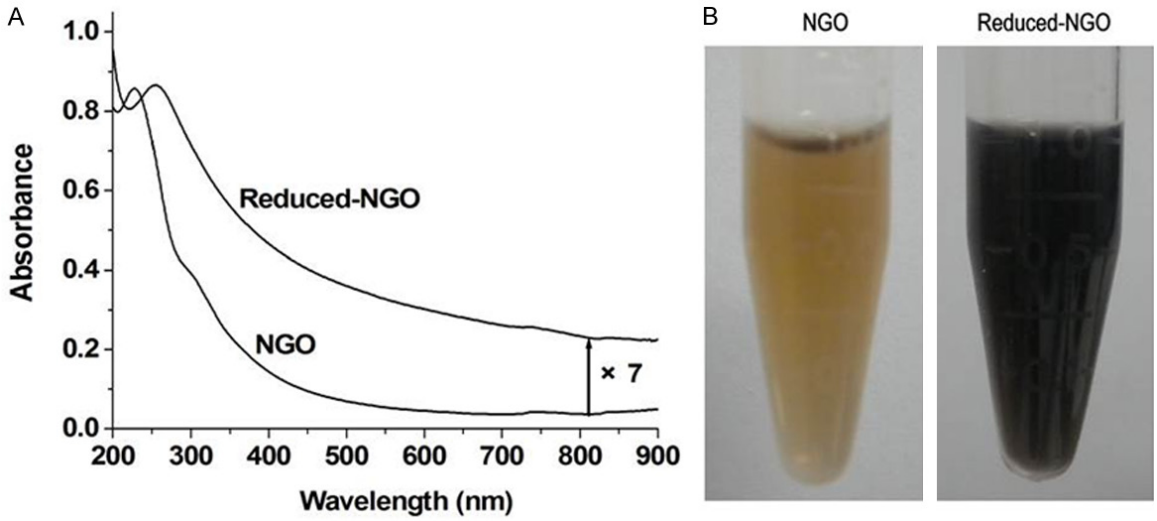

Figure 1. A. The UV-VIS spectra of reduced-NGO. B. The photos of NGO and reduced-NGO solutions.

US), MTT Kit from BioAssay Systems (the US), mica sheet from Electron Microscopy Sciences (the US), DMEM culture solution from GIBCO (the US), and fetal calf serum from Hangzhou SIJIQING Biological engineering Materials Co., Ltd. Human brain astrocytoma and spongioblastoma U87 cells were purchased from the Cell Bank of the Chinese Academy of Sciences (Shanghai, China) and cultured by conventional methods.

Major instruments

An ultrasonic cell disruptor was purchased from Shanghai Zhisun Equipment Co., Ltd., a high speed centrifuge Min1416R from Hema Medical Instrument Co. Ltd, a electric-heated thermostatic water bath DK-S28 from Shanghai Sumsung Laboratory Instrument Co., LTD., an ultraviolet spectrophotometer UV1901PC from Shanghai Aucy Scientific Instrument CO., LTD., a nanosizer Zetasizer APS from Malvern Instruments Ltd. (the US), an atomic force microscope FM-Nanoview 6600 from Suzhou Flyingman Precision Instrument CO., Ltd., a multi-mode microplate reader SpectraMax® i3x from Molecular Devices (Shanghai) and a thermal imager YRH300 from HuaZhi Electronic Technology Co., Ltd. (Zhengzhou).

NGO prepared by hydrazine hydrate reduction method

20 mg NGO platelets were dissolved in 20 ml deionized water. The solution received ultrasonic probe sonography for 3 h and centrifuged at 10000 rpm for 30 min. The resultant supernate, namely, NGO was collected and the sediment was discarded. Afterwards, NGO was prepared into 0.5 mg/ml solution and 20 ul hydrazine hydrate stock solution was added. Then, the mixture was stirred and water bathed for 6 h. After solution being centrifuged at 8000 rpm for 30 min, the supernate was removed and appropriate amount of deionized water was added. The resultant solution was centrifuged again and washed for three times. When the centrifuged sediment was re-suspended by a proper amount of water, 10 mg polyethylene glycol was added. After ultrasonic oscillation for 1 h, the solution was taken out and filtered. The filtrate obtained was reduced-NGO.

Characterization of reduced-NGO

An UV-Vis spectrum was used to detect the absorbance at 200 nm-800 nm before and after the reduction of NGO. Reduced-NGO solution was dripped onto the surface of fresh mica sheet which was dried at 60°C in vacuum for 30 min. An atomic force microscope (AFM) was utilized to detect the morphology of reduced-NGO. The size distribution of reduced-NGO and its average diameter after being placed for different periods of time was detected by a nanosizer.

Test on the photothermal conversion effect of reduced-NGO

Equal volumes of water, NGO and reduced-NGO were put into 1.5 ml EP tubes. Then, these

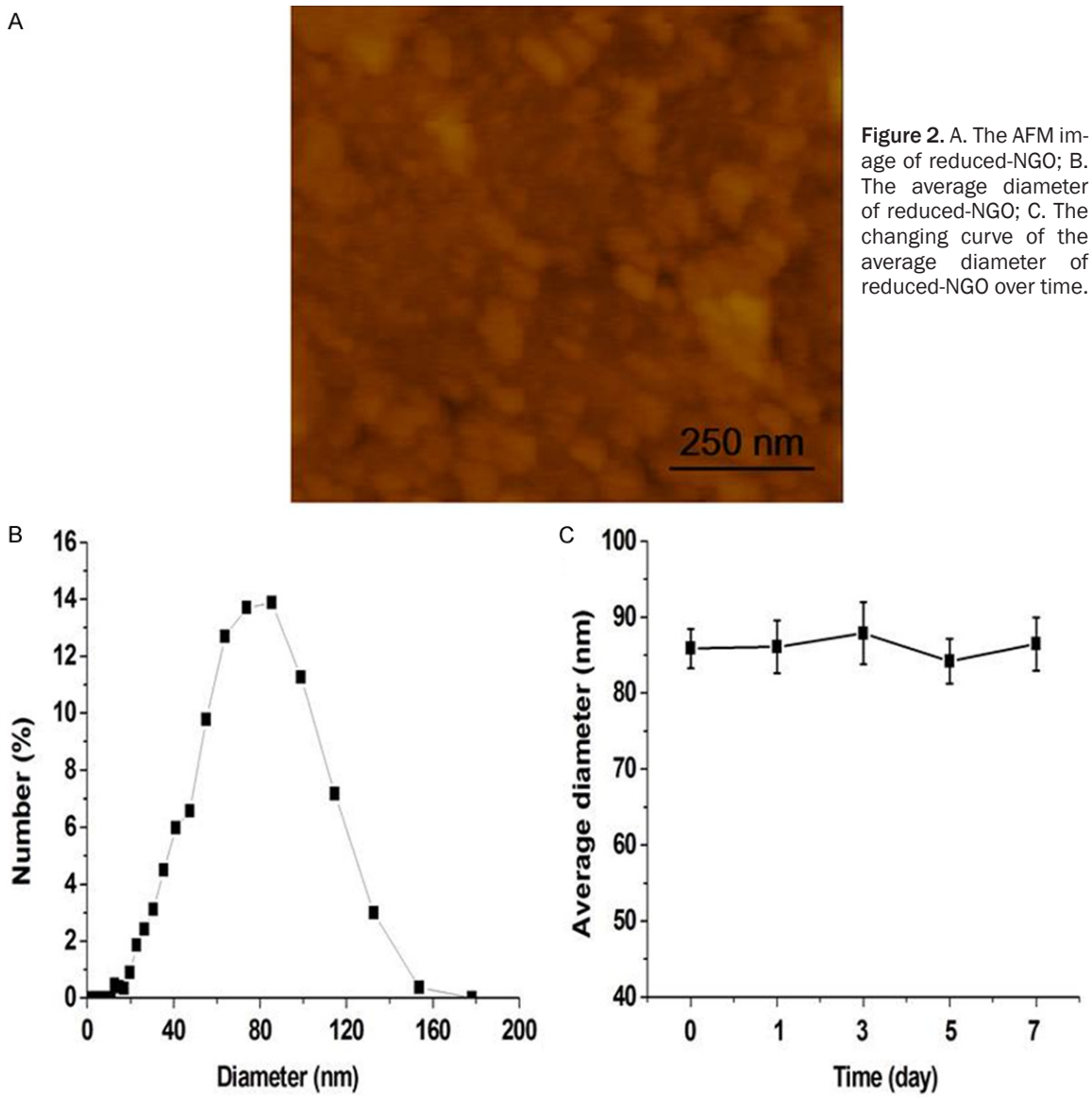

Figure 2. A. The AFM image of reduced-NGO; B. The average diameter of reduced-NGO; C. The changing curve of the average diameter of reduced-NGO over time.

samples were irradiated by 2 w/cm^2 808 nm near-infrared laser and the temperature of the solution was detected every 30 s. In total, the irradiation lasted for 5 min and a temperature-time curve was drawn. In addition, imaging analysis was performed under a thermal imager for these three samples of water, NGO and reduced-NGO.

The photothermal cytotoxicity of reduced-NGO detected by MTT method

Glioma cells during logarithmic phase were collected for digestion, made into cell suspension (10^5/ml), inoculated into a 96-well plate (200 μl per well) and cultured for 24 h. Afterwards, different concentrations of NGO and reduced-NGO were added and the mixture was incubated for another 24 h. Then, the cell culture plate was taken out and the old culture solution was discarded. Later, cells were irradiated by 2 w/cm^2 808 nm near-infrared laser for 5 min. Then, 20 μl culture solution with MTT solution was added in each well. After being cultured in an incubator for 4 h, the supernate was sucked out and 150 ml DMSO was added in each well. At last, the resultant mixture was oscillated in a table concentrator at a low speed for 10 min to dissolve crystal substance in each well adequately and the absorbance (OD value) at 570 nm was detected by a microplate reader.

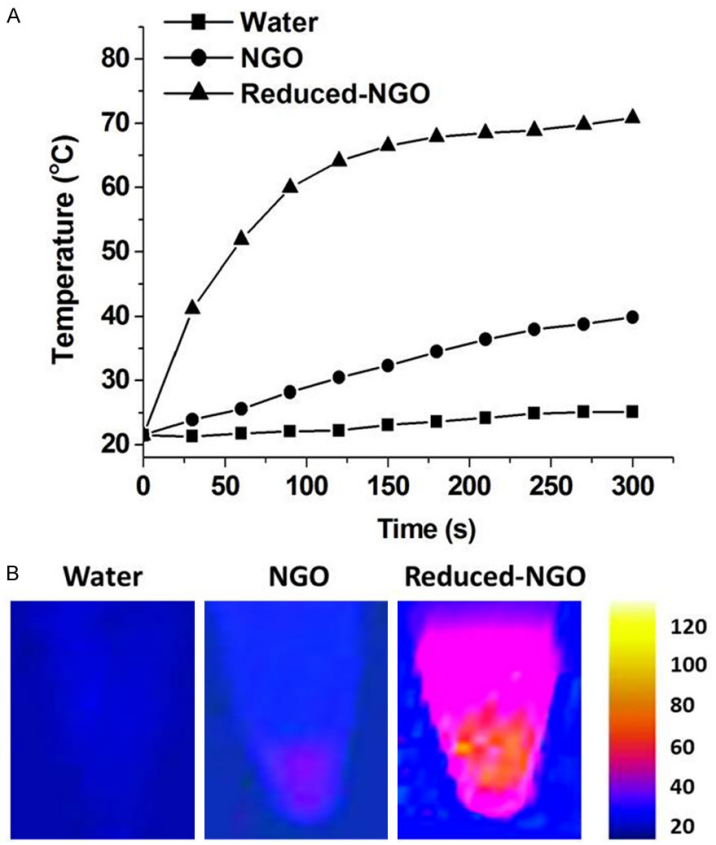

Figure 3. The photothermal conversion effect of reduced-NGO. A. Temperature-time curve; B. Near-infrared thermal imaging pictures.

The construction of a tumor model and the photothermal therapeutic effect of reduced-NGO on tumor

Balb/c nude mice at the age of 3-5 weeks were purchased from Vital River Laboratory Animal Technology Co. Ltd. (with male and female animals randomly distributed). The tumor model was constructed as follows: 100 μL PBS with 1×10^6 U87 cells were injected subcutaneously into the right side of mice's back; these animals were then fed in an animal room. Tumor volume was measured every four days as per the formula. The weight of mice was measured every four days. When tumor volume reached up to about 60 mm^3, mice were divided into five groups-normal saline (control), NGO group, reduced-NGO group, NGO+laser group and reduced-NGO+laser group. Drugs were administered by intratumoral injection. After the completion of treatment, mice were killed and major organs (heart, liver, kidney, spleen and lung) were taken out. Pathological HE section staining was performed with hematoxylin and eosin. Besides, sections were observed under optical microscope and photographed with digital camera.

Statistical analysis

Statistical data were expressed by $\bar{x}\pm s$ and analyzed by a statistical software SPSS13.0. Comparison between groups was conducted by using independent-samples T test. $P<0.05$ meant that there was statistical difference and $P<0.01$ meant that there was significant statistical difference.

Results

The preparation of reduced-NGO

As shown in **Figure 1A**, the UV-Vis absorption spectrum of NGO solution was a smooth curve with only one strong absorbance at 230 nm. After reduction, a red shift was observed for this strong absorbance and the intensity of infrared absorption bands increased about seven times. As shown in **Figure 1B**, the color turned from yellowish-brown to dark black after reduction.

Characterization of the morphology and diameter of reduced-NGO

As shown in **Figure 2A**, reduced-NGO is lamellar particle. The diameter of reduced-NGO detected by nanosizer was 10 nm-160 nm, averaging 89 nm (**Figure 2B**). As shown in **Figure 2C**, after reduced-NGO stood at room temperature for seven days, its average diameter was detected every other day and found to be around 90 nm.

The photothermal conversion effect of reduced-NGO

As shown in **Figure 3**, after NGO and reduced-NGO of the same concentration were irradiated by 808 nm laser (2 w/cm^2), respectively, the temperature of reduced-NGO solution increased rapidly and reached up to 70°C in five minutes, while that of NGO only reached up to 39°C and that of water almost remained at about 22°C (**Figure 3A**). 5 min after irradiation by 808 nm laser (2 w/cm^2), as shown in **Figure 3B** (thermal imaging pictures of water, NGO and

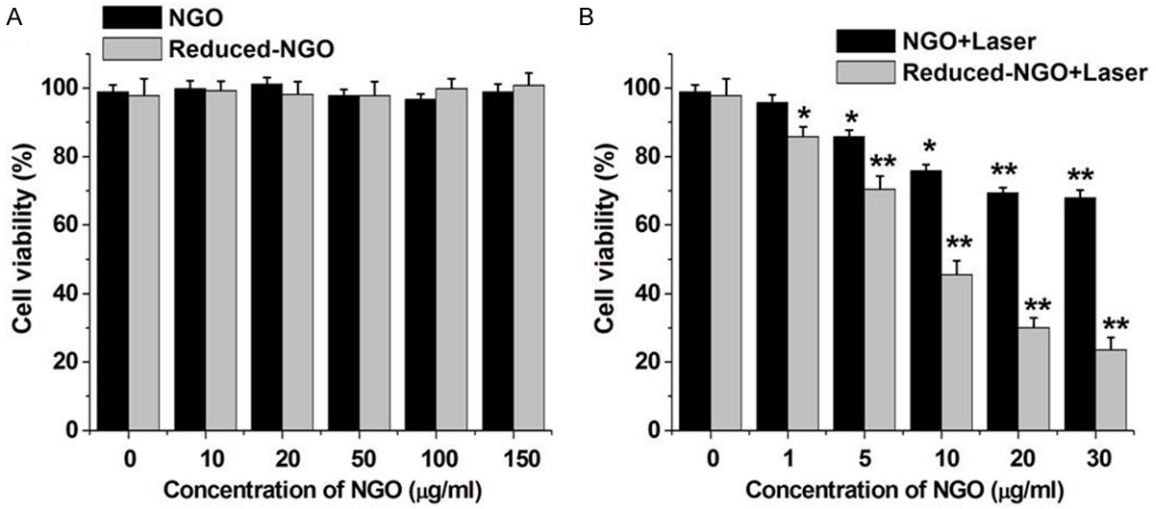

Figure 4. A. The effect of NGO and reduced-NGO on cell viability; B. The effect of NGO and reduced-NGO combined with 808 nm laser on cell viability. *P<0.05, **P<0.01.

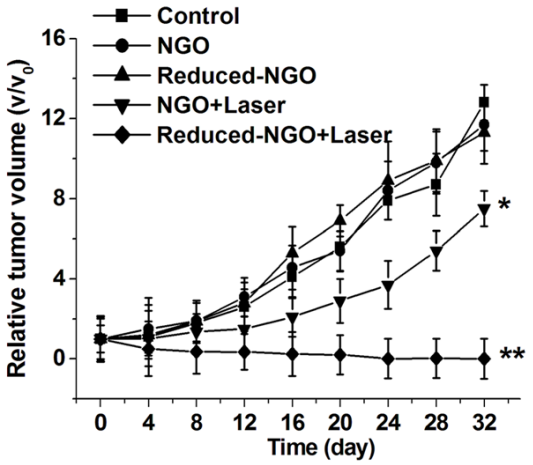

Figure 5. The photothermal therapeutic effect of reduced-NGO. *P<0.05, **P<0.01.

reduced-NGO), the temperature of water, NGO and reduced-NGO reached up to about 20°C, 40°C and above 60°C, respectively.

The cytotoxicity of reduced-NGO

First of all, we detected the effect of NGO and reduced-NGO on cell viability. As shown in **Figure 4A**, both 0-150 ug/ml NGO and reduced-NGO had no significant effect on the viability of U87 cells. Then, 5 min after irradiation by 808 nm laser, as shown in **Figure 4B**, the decrease in cell viability caused by reduced-NGO was more significant compared with that caused by NGO.

The photothermal therapeutic effect of reduced-NGO

As shown in **Figure 5**, after tumor-bearing mice were treated with NGO and reduced-NGO, the tumor inhibition effect was similar to the control group and tumor growth was almost not inhibited. Then, when combined with irradiation by 808 nm laser, NGO slowed down but did not inhibit tumor growth, while reduced-NGO showed significant inhibitory effect.

The toxicity of reduced-NGO in vivo

The toxicity of NGO and reduced-NGO in mice was presented in **Figure 6**. As shown in **Figure 6A**, no significant decrease of weight was observed after mice were treated with NGO or reduced-NGO alone or in combination with laser irradiation. Besides, analysis of HE pathological sections of their major organs indicated that these treatments all had no evident damage to the major organs of mice (**Figure 6B**).

Discussion

In recent years, photothermal therapy, as a new method, became an alternative therapy with little damage for the treatment of tumor. It could kill cells by protein denaturation through increasing temperature up to more than 40°C [18-20]. Common thermal therapies included ultrasound hyperthermia, microwave hyperthermia, endogenetic field hyperthermia, radio-

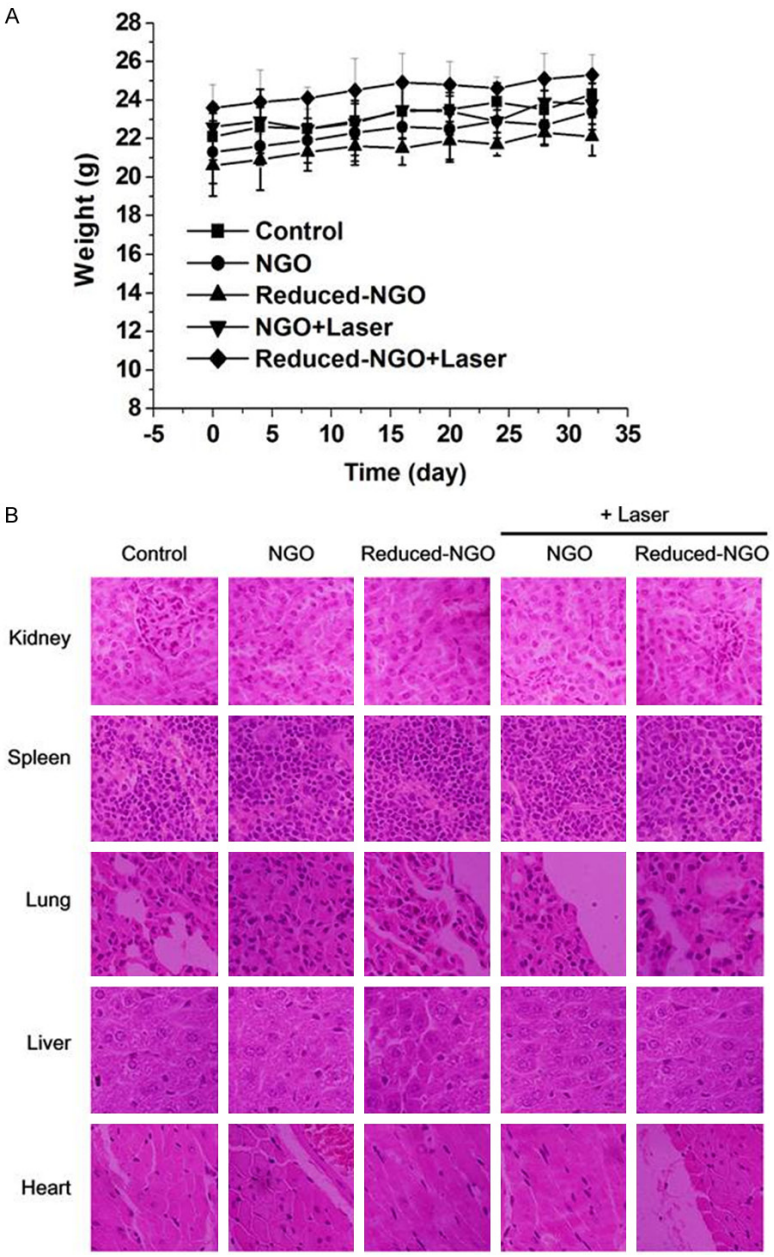

Figure 6. A. Body weight-time curve in mice; B. The H&E staining images of major organs in mice.

frequency hyperthermia, near-infrared photothermal therapy and so forth [21-23]. During thermotherapy, in order to avoid damaging normal tissues caused by hyperthermia, intratumor injection or photothermal targeting preparations were usually used. Among various thermotherapies, laser-induced thermotherapy could kill cells by irradiating light absorbing materials gathering at the tumor site with laser (the light energy was converted into heat energy) [24]. Lasers used in thermotherapy were mainly near-infrared laser. However, since human body had low absorption of NIR, NIR absorbers were needed to enhance thermal damage to the tumor site selectively and improve the therapeutic effect [25-27]. Early studies reported that materials like gold nanorods, AuNCs and gold nanoparticles coated by silicon could absorb near-infrared laser and could be used in tumor diagnosis and photothermal therapy [28].

NGO could be absorbed in the near-infrared region, but its photothermal conversion rate was still low. Nevertheless, studies found that reduced-NGO had evidently stronger NIR absorption intensity and could convert light energy absorbed into heat energy quickly, leading to intracellular protein denaturation. The study results of Yang Kai et al. showed that tumors in mice treated by intratumor injection of reduced-NGO combined with near-infrared laser irradiation obviously scabbed, became smaller and were even eliminated completely after a month. By contrast, NGO combined with laser irradiation failed to eliminate tumors [29].

In this study, reduced-NGO was synthesized by hydrazine hydrate reduction method. Detection by ultraviolet spectrophotometer indicated that the absorption intensity in the near-infrared region of reduced-NGO was seven times stronger than that of NGO. Besides, the color changed from yellowish-brown to dark black, which fully showed that NGP was reduced. It laid a foundation for the application of reduced-NGO in photothermal therapy. Study on *in vitro* photothermal conversion effect showed that the temperature of reduced NGO could reach up to 70°C soon after irradiation

with 2 w/cm^2 near-infrared laser. This temperature was sufficient to make intracellular proteins degenerate. The effect of subsequent *in vivo* and *in vitro* photothermal therapies fully validated this property of reduced-NGO.

In conclusion, reduced-NGO solution was successfully prepared by hydrazine hydrate reduction method. With good stability and biocompatibility, the solution could inhibit tumor growth in combination with near-infrared laser irradiation both *in vivo* and *in vitro*.

Disclosure of conflict of interest

None.

Address correspondence to: Yue-Hong Ma, Pharmacology Teaching and Research Division, College of Basic Medical Sciences, Inner Mongolia Medical University, Jinshan Development Zone, Hohhot, Inner Mongolia Autonomous Region, China. E-mail: mayuehong2010@sina.com

References

[1] Zhu Y, Murali S, Cai W, Li X, Suk JW, Potts JR, Ruoff RS. Graphene and graphene oxide: synthesis, properties, and applications. Adv Mater 2010; 22: 3906-24.

[2] Dreyer DR, Park S, Bielawski CW, Ruoff RS. The chemistry of graphene oxide. Chem Soc Rev 2010 ; 39: 228-40.

[3] Wang K, Jing R, Song H, et al. Biocompatibility of graphene oxide. Nanoscale Research Letters 2011; 6: 1-8.

[4] Sari MM. Fluorescein isothiocyanate conjugated graphene oxide for detection of dopamine. Materials Chemistry & Physics 2013; 138: 843-849.

[5] Rao CN, Sood AK, Subrahmanyam KS, Govindaraj A. Graphene: the new two-dimensional nanomaterial. Angew Chem Int Ed Engl 2009; 48: 7752-77.

[6] Zhou L, Cheng R, Tao H, Ma S, Guo W, Meng F, Liu H, Liu Z, Zhong Z. Endosomal pH-activatable poly (ethylene oxide)-graft-doxorubicin prodrugs: synthesis, drug release, and biodistribution in tumor-bearing mice. Biomacromolecules 2011; 12: 1460-1467.

[7] Hollanda LM, Lobo AO, Lancellotti M, Berni E, Corat EJ, Zanin H. Graphene and carbon nanotube nanocomposite for gene transfection. Mater Sci Eng C Mater Biol Appl 2014; 39: 288-98.

[8] Zhu Y, Murali S, Cai W, Li X, Suk JW, Potts JR, Ruoff RS. Graphene and graphene oxide: synthesis, properties, and applications. Adv Mater 2010; 22: 3906-24.

[9] Compton OC, Nguyen ST. Graphene oxide, highly reduced graphene oxide, and graphene: versatile building blocks for carbon-based materials. Small 2010; 6: 711-723.

[10] Lu XL, Zeng J, Chen YL, He PM, Wen MX, Ren MD, Hu YN, Lu GF, He SX. Sinomenine hydrochloride inhibits human hepatocellular carcinoma cell growth in vitro and in vivo:involvement of cell cycle arrest and apoptosis induction. Int J Oncol 2013; 42: 229-38.

[11] Fabrizio A, Alice F. Liposomes and MTT cell viability assay: An incompatible affair. Toxicol In Vitro 2015; 29: 314-9.

[12] Gunjal PM, Schneider G, Ismail AA, Kakar SS, Kucia M, Ratajczak MZ. Evidence for induction of a tumor metastasis-receptive microenvironment for ovarian cancer cells in bone marrow and other organs as an unwanted and underestimated side effect of chemotherapy/radiotherap. J Ovarian Res 2015; 8: 20.

[13] Liao F, Yang Z, Lu X, Guo X, Dong W. Sinomenine sensitizes gastric cancer cells to 5-fluorouracil in vitro and in vivo. Oncol Lett 2013; 6: 1604-1610.

[14] Sun X, Liu Z, Welsher K, Robinson JT, Goodwin A, Zaric S, Dai H. Nano-graphene oxide for cellular imaging and drug delivery. Nano Res 2008; 1: 203-212.

[15] Lv Y, Li C, Li S, Hao Z. Sinomenine inhibits proliferation of SGC-7901 gastric adenocarcinoma cells via suppression of cyclooxygen-ase-2 expression. Oncol Lett 2011; 2: 741-745.

[16] Jagetia GC. Radioprotection and radiosensitization by curcumin. Adv Exp Med Biol 2007; 595: 301-20.

[17] Robinson JT, Tabakman SM, Yongye L, Wang H, Casalongue HS, Vinh D, Dai H. Ultrasmall reduced graphene oxide with high near-infrared absorbance for photothermal therapy. J Am Chem Soc 2011; 133: 6825-31.

[18] Lin JK, Lin-Shiau SY. Mechanisms of cancer chemoprevention by curcumin. Proc Natl Sci Counc Repub China B 2001; 25: 59-66.

[19] Chignell CF, Bilskj P, Reszka KJ, Motten AG, Sik RH, Dahl TA. Spectral and photochemical properties of curcumin. Photochem Photobiol 1994; 59: 295-302.

[20] Chen TJ, Jeng JY, Lin CW, Wu CY, Chen YC. Quercetin inhibition of ROS-dependent and -independent apoptosis in rat glioma C6 cells. Toxicology 2006; 223: 113-126.

[21] Jiang T, Zhou L, Zhang W, Qu D, Xu X, Yang Y, Li S. Effects of sinomenine on proliferation and apoptosis in human lung cancer cell line NCI-H460 in vitro. Mol Med Rep 2010; 3: 51-6.

[22] Shoeb M, Khan JA, Khan W, et al. ROS-dependent anticandidal activity of zinc oxide nanoparticles synthesized by using egg albumen as a biotemplate. Advances in Natural

Sciences Nanoscience & Nanotechnology 2013; 4: 35015-35026.
[23] Sepúlveda M, Gonano LA, Back TG, Chen SR, Vila Petroff M. Role of CaMKII and ROS in rapid pacing-induced apoptosis. J Mol Cell Cardiol 2013; 63: 135-45.
[24] Pan X, Zhang X, Sun H, Zhang J, Yan M, Zhang H. Autophagy inhibition promotes 5-fluorouraci-induced apoptosis by stimulating ROS formation in human non-small cell lung cancer A549 cells. PLoS One 2013; 8: 55674-56679.
[25] Kuo CT, Hsu MJ, Chen BC, Chen CC, Teng CM, Pan SL, Lin CH. Denbinobin induces apoptosis in human lung adenocarcinoma cells via Akt inactivation, Bad activation, and mitochondrial dysfunction. Toxicol Lett 2008; 177: 48-58.
[26] Yang KC, Uen YH, Suk FM, Liang YC, Wang YJ, Ho YS, Li IH, Lin SY. Molecular mechanisms of denbinobin-induced anti-tumorigenesis effect in colon cancer cells. World J Gastroenterol 2005; 11: 3040-5.
[27] Zhao ZX, Huang YZ, Shi SG, Tang SH, Li DH, Chen XL. Cancer therapy improvement with mesoporous silica nanoparticles combining photodynamic and photothermal therapy. Nanotechnology 2014; 25: 1082-1090.
[28] Hong Y, Yang J, Shen X, Zhu H, Sun X, Wen X, Bian J, Hu H, Yuan L, Tao J, Lei P, Shen G. Sinomenine hydrochloride enhancement of the inhibitory effects of anti-transferrin receptor antibody-dependent on the COX-2 pathway in human hepatoma cells. Cancer Immunol Immunother 2013; 62: 447-54.
[29] Kai Y, Jianmei W, Shuai Z, Tian B, Zhang Y, Liu Z. The influence of surface chemistry and size of nanoscale graphene oxide on photothermal therapy of cancer using ultra-low laser power. Biomaterials 2012; 33: 2206-2214.